認められ（奇異反応），後者によるものと診断した．頭部MRIでは下垂体を含めて脳実質に特記すべき異常はなかった．以上よりばち指を生じる疾患として，内分泌学的異常による末端肥大症は否定的であり，PDPを疑った．

心電図，胸部エックス線検査を行い呼吸器・循環器系疾患の検索を行ったが，正常であった．四肢の骨単純エックス線像では，長管骨骨幹部の骨皮質が肥厚していた．手指において，中手骨・基節骨の骨幹部骨皮質が肥厚していた（図2）．

病理組織学的所見

左前額部の皮膚より生検した．表皮に著変はなかったが，真皮では，肥大した膠原線維と脂腺の過形成，及び汗腺の増加が認められた．膠原線維は皮下脂肪織へも進展し，付属器の上昇がみられた．以上より，真皮が肥厚していると考えた（図3）．増生した膠原線束間には，酸性ムコ多糖と考えられるアルシアンブルー陽性物質が沈着していた（図4）．

血中 **PGE2** 濃度測定

静脈血を採取後（血清分離し），ただちに－80℃保存した．各サンプルは測定時20倍希釈し，PGE2測定ELISAキットにより測定した（Prostaglandin E2 Kit-Monoclonal, Cayman Chemical, USA：京都大学大学院医学研究科皮膚生命科学講座において測定）．患者

血清 PGE2 値は 30 pg/ml であった（健常家族の血清では 29.5 pg/ml）．概ね 1000 pg/ml 以上が異常値であるので正常範囲である．

診断および経過

自験例は，PDP の 3 主徴のうち，ばち指，長管骨を主とする骨膜性骨肥厚，皮膚肥厚性変化を認めた．しかし発症後約 10 年を経た 2010 年 2 月現在でも前額部・頭部にはっきりとした脳回転状皮膚を観察しえなかったため，不全型 PDP と診断した．

PDP の合併症である顔面・胸背部のざ瘡に対しアダパレンを外用しているが，再発・寛解を繰り返している．

考察

自験例は，PDP において合併が知られている貧血などはみられず，家族内発症もなく，いわゆる 3 徴のみで診断した．関節症状のみられる PDP は原発性肥大性骨関節症（primary hypertrophic osteoarthropathy, PHO）とほぼ同義であり，二次性（主に肺性）肥大性骨関節症との鑑別が問題になる．自験例では，内分泌学的異常を伴わず末端肥大症が否定された．また，呼吸器疾患などの基礎疾患もみいだされず，発症が十代であることより，原発性（遺伝性）PDP と診断した．このように PDP は従来，疾患特異的検査が存在しなかったため，時に診断に苦慮する症例があると考えられる．し

かし，2008年原因遺伝子が同定され，新たな展開がみられた．

Uppalら[4]は，パキスタン人PHO家系からNAD(+)-dependent 15-hydroxyprostaglandin dehydrogenase（以下HPGD）遺伝子に変異を見出した．HPGD遺伝子はプロスタグランジンE2（以下PGE2）の分解酵素をコードしており，その欠損により患者血中の過剰に残存したPGE2が尿中に排泄されることも報告された．Uppalらが報告した症例は，いずれも骨病変が顕著な症例であり，Touraineら[2]の提唱した3型のうち，いずれがHPGDの変異により生じる病型なのか，あるいは3つの病型は，同一遺伝子内の変異の位置と関連したものなのか（genotype-phenotype correlation）は未だ明らかになっていない．

Kabashimaら[5]は完全型2例においてHPGD変異の検索および血中PGE2濃度測定を行い，変異は発見されず，PGE2濃度も上昇していなかったことを報告している．彼らの検索した2例はいずれも皮膚肥厚の強い完全型の症例であったことから，HPGDは不全型の一部の症例の原因遺伝子であり，PDPの成因には複数の原因遺伝子が存在すると考察している．自験例においては，皮膚肥厚はあまり強くないが，はっきりとしたばち指と骨膜肥厚があり，不全型と考えられる．しかし，HPGD遺伝子変異例で観察される関節症状はみら

れず，前述のPHOという診断には合致しない．しかし，今後関節症状や頭部脳回転状皮膚の出現があれば病型の再検討をすべきであるが，現在のところ不全型と診断せざるおえない症例と考えられる．なお，過去21年間（1989年以降）の本邦原著論文を検討したが，病型が観察期間中（初診以後）変化したと考えられる症例はみられなかった．完全型，不全型の報告年齢に有意差がなかったので，病型の移行は通常はみられないと推測している．

当該疾患では血中PGE2濃度は異常値を示さなかったが，今後血中・尿中PGE2濃度が病型に関連しているかどうかを検討するためにさらなる症例の集積が待たれる．

本論文の要旨は日本皮膚科学会第826回東京地方会（平成21年9月）において発表した．

文献

1. Friedreich N:Virchows Arch[a] 43:83, 1986

2. Touraine A et al:Presse Med 43:1820, 1935

3. Vague J:Ann Méd 51:152, 1950

4. Uppal S et al:Nat Genet 40:789, 2008

5. Kabashima K et al:Am J Pathol 176:721, 2010

図の説明

図 1

臨床像（手指）.

手指末端は肥大して太鼓ばち状を呈し，爪甲も肥大・彎曲して時計皿様であった.

図 2

単純 X 線像（a:右膝関節・b:右手）.

四肢の長管骨骨幹部骨皮質の肥厚を認めた.手指では，中手骨・基節骨の骨幹部骨皮質の肥厚がみられた.

図 3

病理組織像（左前額部，HE 染色，40 倍）.

真皮内に膠原線維の増生と脂腺の過形成，及び汗腺の増加を認めた.

図 4

病理組織像（左前額部，Alcian Blue 染色，200 倍）.

膠原線維は肥大し，線維束間には青染する物質の沈着がみられる.

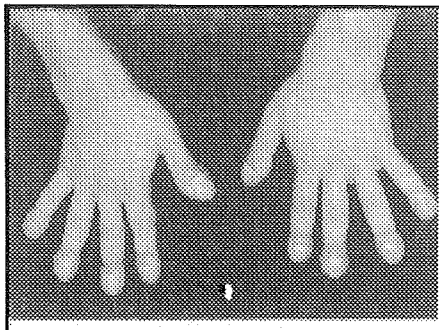

↑
図1
重松

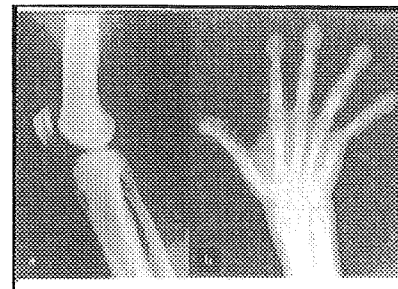

↑
図2
重松

↑
図3
重松

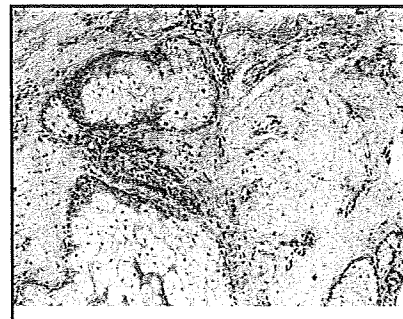

↑
図4
重松

The American Journal of Pathology, Vol. 176, No. 2, February 2010

DOI: 10.2353/ajpath.2010.090454

Epithelial and Mesenchymal Cell Biology

Involvement of Wnt Signaling in Dermal Fibroblasts

Kenji Kabashima,*†‡ Jun-ichi Sakabe,* Ryutaro Yoshiki,* Yasuhiko Tabata,§ Kimitoshi Kohno,¶ and Yoshiki Tokura*

From the Departments of Dermatology and Molecular Biology,¶ School of Medicine, University of Occupational and Environmental Health, Kitakyushu; the Department of Dermatology,† and Center for Innovation in Immunoregulative Technology and Therapeutics,‡ Kyoto University Graduate School of Medicine, Kyoto; and the Institute for Frontier Medical Sciences,§ Kyoto University, Kyoto, Japan*

Pachydermoperiostosis (PDP) is a rare disease characterized by unique phenotypes of the skin and bone, such as thick skin, implying that it may be caused by dysregulation of mesenchymal cells. The aim of this study is to examine the roles of dermal fibroblasts in the pathogenesis of pachydermia in association with Wnt signaling. The numbers of cultured fibroblasts were compared between healthy donors and PDP patients, and mRNA expression profiles in cultured dermal fibroblasts were examined by DNA microarray analysis and real-time reverse transcription-PCR. DKK1 and β-catenin protein expressions were also evaluated by immunohistochemistry in the skin. To evaluate the *in vivo* roles of DKK1 in mice, *DKK1* small interfering RNA was injected to the ears. We found that PDP fibroblasts proliferated more than control fibroblasts and that mRNA expression of a Wnt signaling antagonist, *DKK1*, was much lower in PDP fibroblasts than in normal ones. Consistently, decreased expression of DKK1 in fibroblasts and enhanced expression of β-catenin were noted in PDP patients. Moreover, recombinant human DKK1 protein decreased the proliferation of dermal fibroblasts. In accord with the above human studies, intradermal injections of *DKK1* small interfering RNA into mouse ears increased ear thickness as seen in PDP. Our findings suggest that enhanced Wnt signaling contributes to the development of pachydermia by enhancing dermal fibroblast functions. ***(Am J Pathol 2010, 176:721–732; DOI: 10.2353/ajpath.2010.090454)***

Pachydermoperiostosis (PDP), a form of primary hypertrophic osteoarthropathy, is a rare disease[1–3] diagnosed by the presence of a triad of pachydermia (skin thickening), digital clubbing, and periostosis of long bones. Typically, insidious development of thickening of the fingers and toes, clubbing of the terminal phalanges, enlargement of the hands and feet, hyperhidrosis, increased sebaceous secretion, and velvet coloration of the skin occur mostly in men during adolescence.[4] Radiographic signs of bilateral and symmetrical periostosis are frequently observed as a marked irregular periosteal ossification of the tibias and fibulas.[3] Touraine et al[5] recognized PDP with three clinical presentations or forms: a "complete form" presenting the full-blown phenotype; an "incomplete form" characterized by the phenotype without pachydermia; and a "fruste form" with pachydermia and minimal or absent skeletal changes.

Recently, the incomplete form of PDP, primary osteoarthropathy without pachydermia, was mapped to chromosome 4q33-q34, and gene mutations in *HPGD*, encoding 15-hydroxyprostaglandin dehydrogenase, the main enzyme of prostaglandin (PG) degradation, were identified.[6] Therefore, it has been suggested that the digital clubbing and bone changes are due to elevated PGE_2. However, the pathomechanism underlying pachydermia of PDP remains unknown.

Since the major manifestations of complete PDP occur in both skin and bone, the etiology could be related to the dysregulation of bone morphogenetic proteins (BMP), transforming growth factor (TGF)-β, and/or wingless (Wnt) pathways.[7–9] The Wnt signaling consists of canonical and non-canonical pathways. The canonical pathway involves cytosolic β-catenin stabilization, nuclear translocation and gene regulation, and the non-canonical pathways activate rho, rac, JNK, and protein kinase C.[10,11] These signaling pathways are mediated by Wnt protein, which binds to a frizzled Wnt receptor. Wnt signaling is modulated by several different families of

Supported in part by grants from the Ministry of Education, Culture, Sports, Science and Technology and the Ministry of Health, Labour and Welfare of Japan.

K.K. and J.S. contributed equally to this work.

Accepted for publication October 20, 2009.

Address reprint requests to Dr. Kenji Kabashima, Department of Dermatology, Kyoto University Graduate School of Medicine, 54 Shogoin Kawaracho, Sakyo-ku, Kyoto 606-8507, Japan. E-mail: kaba@kuhp.kyoto-u.ac.jp.

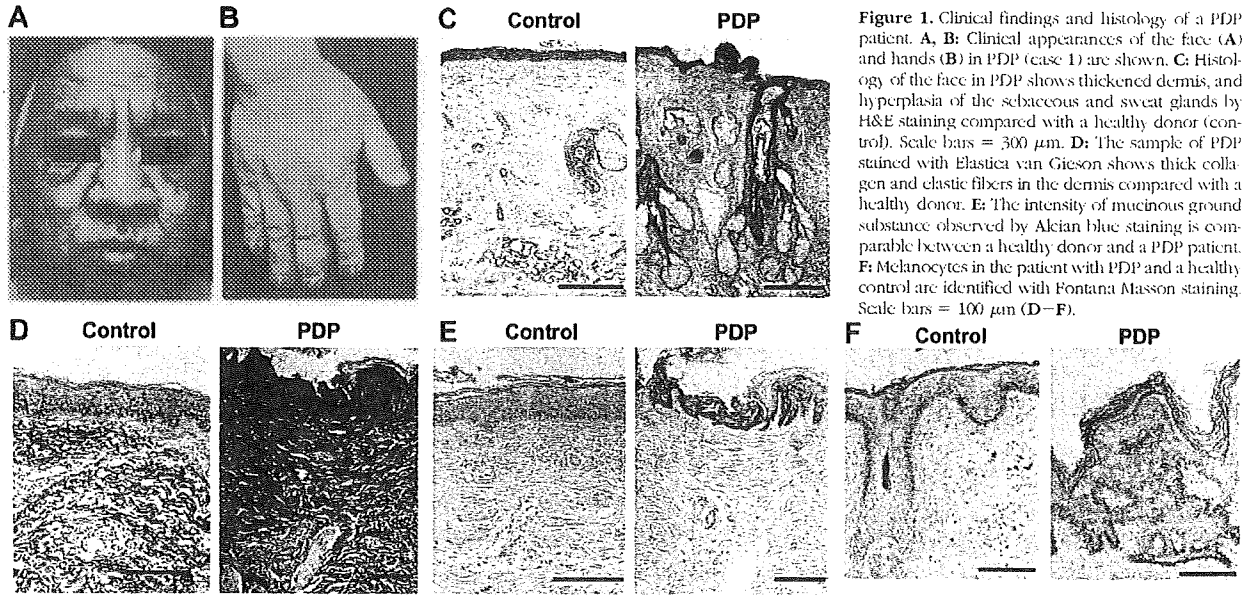

Figure 1. Clinical findings and histology of a PDP patient. **A, B:** Clinical appearances of the face (**A**) and hands (**B**) in PDP (case 1) are shown. **C:** Histology of the face in PDP shows thickened dermis, and hyperplasia of the sebaceous and sweat glands by H&E staining compared with a healthy donor (control). Scale bars = 300 μm. **D:** The sample of PDP stained with Elastica van Gieson shows thick collagen and elastic fibers in the dermis compared with a healthy donor. **E:** The intensity of mucinous ground substance observed by Alcian blue staining is comparable between a healthy donor and a PDP patient. **F:** Melanocytes in the patient with PDP and a healthy control are identified with Fontana Masson staining. Scale bars = 100 μm (**D**–**F**).

secreted down-regulators. Among them, Dickkopf (DKK) is a family of cysteine-rich proteins comprising at least four different forms (DKK1, DKK2, DKK3, and DKK4), which are coordinately expressed in mesodermal lineages. The best studied of these is DKK1, which blocks the canonical Wnt signaling by inducing endocytosis of lipoprotein receptor-related protein 5/6 (LRP5/6) complex[12] without affecting the frizzled Wnt receptor.[13] DKK1 induces the formation of ectopic heads in *Xenopus laevis* in the presence of BMP inhibitors[14] and modulates apoptosis during vertebrate limb development.[15] High mRNA levels of *DKK1* in human dermal fibroblasts of the palms and soles inhibit the function and proliferation of melanocytes via the suppression of β-catenin and microphthalmia-associated transcription factor.[16,17] In parallel, DKK1 transgenic mice under the control of keratin 14 have no pigmentation on the trunk because of the absence of melanocytes in the inner-follicular epidermis, as well as the lack of hair follicle development.[18] These findings suggest that DKK1 is deeply involved in the formation and differentiation of the skin.

Here we investigated two complete cases of PDP using dermal fibroblasts to address the pathogenetic mechanisms. DNA microarray analysis revealed that the proliferation of primary fibroblasts of PDP was increased with decreased expression of *DKK1* mRNA in cultured fibroblasts. Consistent with this finding, immunohistochemistry indicated decreased expression of DKK1 in fibroblasts and enhanced expression of β-catenin in the skin of patients with PDP, suggesting that Wnt signaling is enhanced in PDP. The intradermal injection of *DKK1* synthetic small interfering RNA (siRNA) increased the ear thickness of mice as seen in PDP. These results suggest that enhanced Wnt signaling contributes to the development of pachydermia.

Materials and Methods

Patients

Case 1

A 50-year-old male was referred to our clinic. The skin on his head and face was thick and oily with a dark velvet color. Naso-labial folds and transverse furrowing of the forehead were prominent (Figure 1A). The hands were enlarged with marked clubbing of the second and fifth digits, as compared with those of an age- and sex-matched healthy donor (Figure 1B). These symptoms developed when he was 18 years old. X-ray examination of the long bones showed major periostosis with cortical thickening and widening of the shafts (data not shown). Histology of the skin showed thickened dermis, and sebaceous and sweat gland enlargement, as compared with that of a healthy control (Figure 1C). Elastica van Gieson staining showed thick and interwoven collagen bundles in some areas of the dermis and also thick and partially fragmented elastic fibers in PDP (Figure 1D). The intensity of mucinous ground substance observed by Alcian blue staining was comparable between a healthy control and a PDP patient (Figure 1E). On the other hand, Fontana Masson staining revealed that the number of melanocytes and the intensity of the staining in the patient with PDP was higher than that in a healthy control (Figure 1F). Neither hepatosplenomegaly nor internal malignancy was found on physical examination or computed tomography scans. Biochemical tests showed normal levels of thyroid-stimulating hormone and growth hormone, which likely rules out thyroid acropathy and acromegaly. Family history was noncontributory. Based on these clinical manifestations and histological findings, the patient was diagnosed as the complete form of PDP

Case 2

The patient was a 38-year-old male with clinical findings similar to case 1, including pachydermia, digital clubbing, and periostosis. He had no signs or symptoms of hepatosplenomegaly, pulmonary diseases, tumoral syndrome, thyroid acropathy, or acromegaly (data not shown) as reported previously.[19]

Cell Preparation, Culture, and Reagents

Skin biopsies of the right temple (case 1) and scalp (case 2) were performed for histology and primary culture of fibroblasts. Control donors were matched for age, sex, and biopsy site, and the samples were processed in parallel. Institutional approval and informed consent were obtained from all subjects. The biopsy samples were immersed in Dulbecco's Modified Eagle Medium (Sigma, St. Louis, MO) containing 10% heat-inactivated fetal calf serum (Invitrogen, Carlsbad, CA), 5×10^{-5} mol/L 2-mercaptoethanol, 2 mmol/L L-glutamine, 25 mmol/L HEPES (Cellgro, Herndon, VA), 1 mmol/L nonessential amino acids, 1 mmol/L sodium pyruvate, 100 units/ml penicillin, and 100 μg/ml streptomycin, with 5% CO_2 at 37°C. The fibroblasts were allowed to adhere to the surface of 100-mm plastic tissue culture dishes (Nunc, Roskilde, Denmark). To evaluate the number of fibroblasts, 2×10^5 third-passage fibroblasts were seeded in 1 ml of medium in 24-well dishes and resuspended with trypsin/EDTA 1 week later. The numbers of fibroblasts were evaluated 7 and 14 days after seeding by flow cytometry using FACSCanto (BD Biosciences, San Diego, CA) with standard beads Flow Count (Beckman Coulter, Fullerton, CA) as per the manufacturer's instructions. The actin bundle formation of cultured fibroblasts from a healthy individual and an individual with PDP were examined by staining with alexa 488-labeled phalloidin antibody (Invitrogen) 5 days after the fourth passage.

For treatment with DKK1, fibroblasts were harvested 5 days after a comparable number of passages and cultured again at 1×10^6 cells in one ml of medium with or without recombinant human DKK1 (R&D Systems Inc., Minneapolis, MN) for another 2 days. For treatment with PGE_2, fibroblasts were harvested 5 days after a comparable number of passages and cultured again at 1×10^5 cells in two ml of medium with or without PGE_2 (Sigma) in the presence of indomethacin (10 μmol/L; Cayman Chemical Co., Ann Arbor, MI) for another 4 days.

Flow Cytometry and Histology

Flow cytometric analysis was performed with doublet discrimination on the FACSCanto[20] and FlowJo software (TreeStar, San Carlos, CA).[21] Human fibroblasts were treated with cytofix/cytoperm buffer according to the manufacturer's protocol (BD Biosciences). For cell cycle analysis, fibroblasts were incubated with 7-amino actinomycin D (7-AAD) (BD Biosciences) for 20 minutes at 4°C. After staining with 7-AAD, the DNA contents were analyzed by flow cytometry. For β-catenin staining, fibroblasts were stained with phycoerythrin-labeled β-catenin antibody (H-102, Santa Cruz Biotechnology Inc., Santa Cruz, CA), and mean fluorescence intensity was evaluated by flow cytometry.

For histology, the biopsy samples and the ears of mice were fixed in 10% formaldehyde. Sections of 5-μm thickness were prepared and stained with H&E, Elastica van Gieson, or Alcian blue. Immunohistochemical staining on paraffin-embedded sections was performed using a Vectastain ABC kit (Vector Laboratories, Burlingame, CA).[20] Antibodies used were rabbit anti-human polyclonal DKK1 (ab61034, Abcam, Cambridge, UK), mouse monoclonal anti-human β-catenin IgG1 (610153, BD Biosciences, San Diego, CA), and rabbit anti-human polyclonal proliferating cellular nuclear antigen antibodies (SC-7907, Santa Cruz Biotechnology Inc., Santa Cruz, CA). The control antibodies used were rabbit non-immune serum or mouse IgG1 (X0931, Dako, Glostrup, Denmark). The immunoreactivity was visualized by Fast Red or diaminobenzidine (Sigma), and the sections were then counterstained with hematoxylin. Images were acquired on a 600CL-CU cooled charge-coupled device video camera (Pixera, Los Gatos, CA) and processed with InStudio 1.0.0 (Pixera).

Western Blot Analysis

For Western blotting studies, fibroblasts were isolated from a healthy donor. Cytoplasm- and nuclear- proteins were extracted by NucBuster Protein Extraction Kit (Novagen, Darmstadt, Germany). Twenty μg protein samples were electrophoresed by 8% SDS-polyacrylamide gel electrophoresis and electroblotted onto polyvinylidene difluoride membranes for 2 hours at 180 mA. After blocking with 5% skim milk solution, the membranes were incubated with rabbit anti-human β-catenin (SC-7199; 1:1000, Santa Cruz Biotechnology Inc.) polyclonal antibodies or rabbit anti-human glyceraldehyde-3-phosphate dehydrogenase (SC-25778; 1:1000, Santa Cruz Biotechnology Inc.) antibody and detected with horseradish peroxidase-conjugated goat anti-rabbit IgG (Bio-Rad, Hercules, CA). Immunoblots were visualized using the ECL Plus Western Blotting Detection Reagents (GE Health care, Buckinghamshire, UK) according to the manufacturer's protocol. Bands were quantified by densitometry with the help of a CS Analyzer ver. 2.0 (ATTO, Tokyo, Japan).

Quantitative Reverse Transcription-PCR and Microarray Procedures

Total RNA was extracted from three-passage fibroblasts (case 1 and the control) cultured for 2 days with the RNeasy Mini Kit (QIAGEN, Valencia, CA). cDNA was reverse transcribed from total RNA samples using the TaqMan Reverse Transcription (RT) reagents (Applied Biosystems, Foster City, CA). Human *DKK1* (Assay ID: Hs00183740) mRNA expression was quantified using TaqMan Gene Expression Assay (Applied Biosystems) with the ABI PRISM 7700 sequence detection system (Applied Biosystems). As an endogenous reference for these RT-PCR quantification studies, human *GAPDH* con-

Table 1. PCR and Sequencing Primers

PCR Primer	Sequence	Tm	Binding site
hDKK1-Exon1, 2			
Forward	5′-CGTCTGCTATAACGCTCGCTGGTAG-3′	77	Promoter
Reverse	5′-AATTCATAGACGCTCAAAGGCTGGA-3′	73	Intron2
hDKK1-Exon3, 4			
Forward	5′-ACTTGCCCCTACCACAGTTG-3′	70	Intron2
Reverse	5′-GTTCCTGCCAATCACCAAGT-3′	68	3′UTR
hTCF-4-Exon1			
Forward	5′-TGGCTTTTCTTCCTCCTTCA-3′	66	5′UTR
Reverse	5′-AGAAAAAGAATCGGCGAGGT-3′	66	Intron1
hTCF-4-6			
Forward	5′-GCGATTTCTGGCAGGTAGTC-3′	70	Intron7
Reverse	5′-TAGCGATCCAGGAAGATGCT-3′	68	Intron10
hTCF-4-9			
Forward	5′-TTAGTAGGGGTTGGGGGAAG-3′	70	Intron13
Reverse	5′-TTGGTAGAATCATGAGGTTCTTCTC-3′	71	3′UTR
hHPGD Exon1			
Forward	5′-GCTGGCTTGACAGTTTCCTC-3′	70	5′UTR
Reverse	5′-CAGCCTCAGCTTCAGCAAAT-3′	68	Intron1
hHPGD Exon2			
Forward	5′-TTGCTGAAGCTGAGGCTGT-3′	68	Intron1
Reverse	5′-TCTTGCCTTTCTTTCGGTTT-3′	64	Intron2
hHPGD Exon3			
Forward	5′-TCCACAAACCACACATTGAGA-3′	67	Intron2
Reverse	5′-CCAGCTTTCTGTAACTTCCCTTT-3′	70	Intron3
hHPGD Exon4			
Forward	5′-TAGGCAAACCCAAAGAATCC-3′	66	Intron3
Reverse	5′-CACATGGGAGCAGAGACATC-3′	70	Intron4
hHPGD Exon5			
Forward	5′-CCTGGGGAGGCAGAAAAA-3′	67	Intron4
Reverse	5′-TTTATTTGGTTCTTTATGTGATCTGA-3′	67	Intron5
hHPGD Exon6			
Forward	5′-TGCAGAGTTCAGTAGATAAGAGAAGC-3′	73	Intron5
Reverse	5′-TGCTTGGAATTTAGGCAGAGA-3′	67	Intron6
hHPGD Exon7			
Forward	5′-TTGGAAGTAGCAATAGTTTAATGA-3′	68	Intron6
Reverse	5′-TCACCAAGTGCATGAAGGAA-3′	66	3′UTR

Sequencing Primer	Sequence	Binding site
hDKK1-Exon1, 2		
Forward	5′-CGTCTGCTATAACGCTCGCTGGTAG-3′	Promoter
Reverse	5′-AATTCATAGACGCTCAAAGGCTGGA-3′	Intron2
hDKK1-Exon1-S2		
Forward	5′-CCACCTTGAACTCGGTTCTC-3′	Exon1
hDKK1-Exon2-S1		
Forward	5′-AGAACGTGCTGAATGTGTGC-3′	Intron1
hDKK1-Exon3, 4		
Forward	5′-ACTTGCCCCTACCACAGTTG-3′	Intron2
Reverse	5′-GTTCCTGCCAATCACCAAGT-3′	3′UTR
hDKK1-Exon3-S1		
Forward	5′-CCTTGGATGGGTATTCCAGA-3′	Exon3
hDKK1-Exon4-S1		
Forward	5′-TCATCAGACTGTGCCTCAGG-3′	Exon4
hDKK1-Exon4-S2		
Forward	5′-AAGGTGCTGCACTGCCTATT-3′	3′UTR
hTCF-4-Exon1		
Forward	5′-TGGCTTTTCTTCCTCCTTCA-3′	5′UTR
Reverse	5′-AGAAAAAGAATCGGCGAGGT-3′	Intron1
hTCF-4-Exon9		
Forward	5′-GCTTGGGGGTTATGAGACAA-3′	Intron8
Reverse	5′-AGACATTCTGCCACCTGACC-3′	Intron9
hTCF-4-Exon10		
Forward	5′-CCTTGGCGTAATGTGTGATG-3′	Intron9
Reverse	5′-TAGCGATCCAGGAAGATGCT-3′	Intron10
hTCF-4-Exon14		
Forward	5′-ACATCCCTTAGGTGACCTCA-3′	Intron13
Reverse	5′-GGGGGCAAATTAAGAAAAGTG-3′	3′UTR

(table continues)

Table 1. *Continued*

Sequencing Primer	Sequence	Binding site
hHPGD Exon1		
Forward	5′-GCTGGCTTGACAGTTTCCTC-3′	5′UTR
Reverse	5′-CAGCCTCAGCTTCAGCAAAT-3′	Intron1
hHPGD Exon2		
Forward	5′-TTGCTGAAGCTGAGGCTGT-3′	Intron1
Reverse	5′-TCTTGCCTTTCTTTCGGTTT-3′	Intron2
hHPGD Exon3		
Forward	5′-TCCACAAACCACACATTGAGA-3′	Intron2
Reverse	5′-CCAGCTTTCTGTAACTTCCCTTT-3′	Intron3
hHPGD Exon4		
Forward	5′-TAGGCAAACCCAAAGAATCC-3′	Intron3
Reverse	5′-CACATGGGAGCAGAGACATC-3′	intron4
hHPGD Exon5		
Forward	5′-CCTGGGGAGGCAGAAAAA-3′	Intron4
Reverse	5′-TTTATTTGGTTCTTTATGTGATCTGA-3′	Intron5
hHPGD Exon6		
Forward	5′-TGCAGAGTTCAGTAGATAAGAGAAGC-3′	Intron5
Reverse	5′-TGCTTGGAATTTAGGCAGAGA-3′	Intron6
hHPGD Exon7		
Forward	5′-TTGGAAGTAGCAATAGTTTAATGA-3′	Intron6
Reverse	5′-TCACCAAGTGCATGAAGGAA-3′	3′UTR

The exons of DKK1, TCF7L2 (TCF-4), and HPGD genes were amplified via PCR in a thermal cycler using the forward and reverse primer pairs indicated in the upper list. Direct sequencing was performed with the BigDye Terminator v3.1 Cycle Sequencing Kit and sequencing primers indicated in the lower list. Binding sites of primers are also indicated.

trol reagents (Assay ID: Hs99999905) (Applied Biosystems) were used. The relative expression was calculated using the ΔΔ Ct method.[22]

For DNA microarray analysis, total RNAs were extracted from fibroblasts with the RNeasy Mini Kit (QIAGEN). For transcriptomic profiling, we used an oligonucleotide-based DNA microarray, AceGene (HumanOligoChip30K, DNA Chip Research, Yokohama, Japan). Images were analyzed with DNASIS Array (Hitachi Software Engineering, Tokyo, Japan), according to the manufacturer's instructions. Mean and SD of background levels were calculated, and genes with intensities less than mean plus 2SD of background levels were excluded from further analysis. The Cy5/Cy3 ratios of all spots on the DNA microarray were normalized by the method of global normalization.

Genetic Analysis for DKK1, TCF, *and* HPGD

Three healthy controls and two PDP patients (cases 1 and 2) were enrolled and followed up according to local

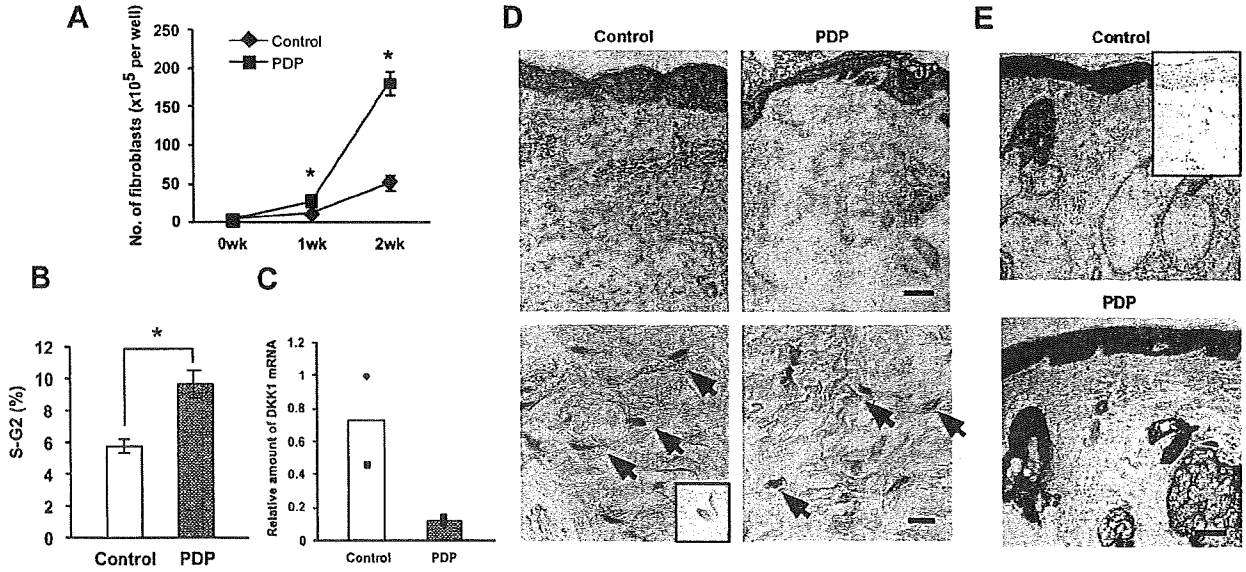

Figure 2. Characteristics of dermal fibroblasts and histology of the skin in PDP. **A:** Fibroblasts from a healthy individual (control) and an individual with PDP (case 1) (PDP) were incubated and the numbers of fibroblasts examined. **B:** The percentages of fibroblasts in S-G2 phase are shown. **C:** The levels of *DKK1* mRNA in fibroblasts from two controls and two PDPs were normalized against GAPDH, and the level of one of the control *DKK1* mRNAs is regarded as one. Filled symbols indicate two independent individuals and columns represent the average. **D** and **E:** Skin sections were stained with anti-human DKK1 (**D**) and β-catenin (**E**) antibodies. **Arrows** show the perinuclear area of fibroblasts (**D**). Scale bars: upper panels (150 μm), and lower panels, 10 μm (**D**), and 100 μm (**E**). We include that the controls incorporating non-immune serum (**D**) or mouse IgG1 (**E**) as insets show no specific reactivity. The student's *t* test was performed (*$P < 0.05$) (**A**, **B**).

Table 2. DNA Microarray Analysis

Gene names	Accession ID	Expression levels		Difference	Fold difference
		Control	PDP		
BMP2	NM_001200_1	5.72	5.87	0.16	–
BMP3	M22491_1	ND	ND	NA	–
BMP4	NM_001202_1	7.20	7.46	0.26	–
BMP5	NM_021073_1	4.61	4.30	−0.30	–
BMP6	NM_001718_1	4.34	4.96	0.61	–
BMP7	NM_001719_1	ND	ND	NA	–
BMP8B	NM_001720_1	5.47	5.65	0.18	–
BMP10	NM_014482_1	ND	ND	NA	–
BMP15	NM_005448_1	ND	ND	NA	–
TGFB1	NM_000660_1	8.87	7.91	−0.97	–
TGFB2	NM_003238_1	4.34	5.05	0.72	–
TGFBR1	NM_004612_1	ND	ND	NA	–
TGFBR2	NM_003242_1	ND	ND	NA	–
TGFBR3	NM_003243_1	4.34	4.51	0.17	–
WNT1	NM_005430_1	6.66	5.45	−1.21	0.4
WNT2	ENSG00000105989	ND	ND	NA	–
WNT2B	NM_024494_1	6.36	6.95	0.60	–
WNT4	AY009398_1	4.33	4.35	0.03	–
WNT5A	NM_003392_1	5.36	5.85	0.50	–
WNT6	BC004329_1	5.13	4.99	−0.14	–
WNT7A	NM_004625_1	ND	ND	NA	–
WNT8B	NM_003393_1	7.27	6.88	−0.39	–
WNT9A	AB060283_1	7.36	6.92	−0.44	–
WNT9B	AF028703_1	5.69	4.47	−1.22	0.4
WNT10A	NM_025216_1	4.40	5.40	1.00	–
WNT10B	NM_003394_1	5.73	4.48	−1.25	0.4
WNT11	NM_004626_1	6.46	5.85	−0.61	–
WNT16	NM_016087_1	7.63	6.80	−0.83	–
FZD1	NM_003505_1	7.19	6.91	−0.28	–
FZD2	AB017364_1	7.05	7.01	−0.03	–
FZD3	AJ272427_1	7.51	6.85	−0.67	–
FZD3	NM_017412_1	ND	ND	NA	–
FZD4	NM_012193_1	6.09	6.49	0.41	–
FZD5	NM_003468_1	5.02	5.44	0.42	–
FZD6	NM_003506_1	5.95	6.37	0.42	–
FZD7	NM_003507_1	9.32	9.40	0.08	–
FZD8	AB043703_1	ND	ND	NA	–
DKK1	NM_012242_1	11.61	8.46	−3.15	0.1
DKK2	NM_014421_1	6.53	6.93	0.40	–
DKK3	NM_015881_1	9.24	9.15	−0.08	–
KREMEN1	AB059618_1	ND	ND	NA	–
KREMEN2	NM_024507_1	5.20	4.33	NA	–
COL1A1	K03179_1	7.57	7.90	0.34	–
COL1A2	NM_000089_1	13.54	13.98	0.44	–
COL2A1	NM_033150_1	9.46	10.09	0.63	–
COL3A1	NM_000090_1	10.26	11.43	1.17	2.3
COL4A1	NM_001845_1	8.66	7.83	−0.83	–
COL4A2	X05562_1	7.17	6.83	−0.34	–
COL4A3	U02519_1	4.54	5.04	0.49	–
COL4A4	NM_000092_1	4.73	4.30	−0.43	–
COL4A5	NM_000495_1	4.23	5.72	1.50	2.8
COL4A6	D63562_1	8.41	8.68	0.28	–
COL5A1	BC008760_1	10.35	10.25	−0.09	–
COL5A3	NM_015719_1	5.57	6.20	0.62	–
COL6A2	AY029208_1	10.90	10.62	−0.29	–
COL6A3	NM_004369_1	6.64	5.37	−1.27	0.4
COL8A1	NM_001850_1	10.47	11.09	0.61	–
COL8A2	M60832_1	5.43	5.55	0.11	–
COL9A1	NM_001851_1	6.97	6.84	−0.13	–
COL9A2	NM_001852_1	4.15	6.13	1.98	4
COL9A3	NM_001853_1	4.73	5.17	0.44	–
COL10A1	NM_000493_1	4.10	6.90	2.80	7
COL11A1	NM_001854_1	6.45	9.28	2.84	7
COL11A2	J04974_1	ND	ND	NA	–
COL12A1	NM_004370_1	4.98	6.26	1.27	2.5

(*table continues*)

Table 2. *Continued*

Gene names	Accession ID	Expression levels		Difference	Fold difference
		Control	PDP		
COL14A1	Y11711_1	4.21	5.81	1.60	3
COL15A1	NM_001855_1	ND	ND	NA	–
COL17A1	NM_000494_1	4.32	6.33	2.01	4
COL18A1	NM_030582_1	5.73	6.03	0.30	–
COL19A1	NM_001858_1	ND	ND	NA	–
FN1	X07717_1	7.10	6.69	−0.41	–
FN5	NM_020179_1	6.41	6.71	0.30	–
ELN	NM_000501_1	7.60	7.33	−0.26	–

The upper list of genes related to BMP, TGF-β, and Wnt signaling. The lower list of genes is related to collagens, fibronectins, and elastin. The mRNA expression levels of a healthy donor (control) and the individual with PDP (PDP) are normalized by LOWESS normalization, and indicated by log2. The values in Difference indicate mRNA expression levels of the individual with PDP—those of the healthy individual. The values under &lquote;Fold Difference' indicate mRNA expression levels of the individual with PDP/those of the healthy individual, ie, Log2(Difference). The symbol "−" in the Fold Difference indicates non-significant difference between the healthy donor and the individual with PDP. ND, not determined. NA, not applicable

ethical guidelines. Genomic DNA was isolated from primary fibroblasts or peripheral blood leukocytes using proteinase K and the PCI (phenol/chloroform/isoamyl alcohol) extraction procedure. The *DKK1* (GenBank: NM012242), *TCF7L2* (*TCF-4*) (GenBank: NM030756), and *HPGD* (NM000860) genes were amplified via PCR in a thermal cycler (Eppendorf, Hamburg, Germany) using forward and reverse primer pairs (Table 1).

Amplified products were purified with the QIAquick Gel Extraction Kit (QIAGEN, Valencia, CA) or Wizard SV Gel and PCR Clean-Up System (Promega, Madison, WI) after 1.5% agarose electrophoresis. Direct sequencing was performed with the BigDye Terminator v3.1 Cycle Sequencing Kit (Applied Biosystems, Foster City, CA) and sequencing primers (Table 1) using capillary electrophoresis (ABI Prism 3130xl Genetic Analyzer; Applied Biosystems), and analyzed with ABI Prism DNA Sequencing Analysis software ver. 5.1 (Applied Biosystems) as previously described.[23]

Application of Mouse DKK1 siRNA

Mouse *DKK1* siRNA (5′-GAA CCA CAC UGA CUU CAA ATT-3′) was purchased from Nippon EGT (Toyama, Japan). siRNA duplexes were generated by mixing sense and antisense single-stranded RNA oligomers equally in an annealing buffer (NIPPON EGT).[24] Negative control siRNA (AM4611) was purchased from Ambion (Austin, TX). To impregnate mouse *DKK1* siRNA into cationized gelatin microspheres,[25] 10 μl of PBS solution (pH 7.4) containing 10 μg of mouse *DKK1* siRNA was dropped onto 1 mg of the freeze-dried cationized gelatin microspheres, kept overnight at 4°C, and added to 190 μl of PBS. Ten μl of this siRNA solution was injected intradermally into the center of the ears of 8-week-old C57BL/6j female mice (obtained from SLC, Shizuoka, Japan) using a 30-gauge needle four times every 7 days. The same amount of cationized gelatin-conjugated nonsense siRNA was applied as a negative control. The ear thickness was measured before each injection and one week after the last injection using dial-thickness gauge (PG-01, TECLOCK, Okaya, Japan). The injected area was sampled for histology and RT-PCR analysis using 6-mm punch biopsy. Mice were maintained on a 12-hour light/dark cycle under specific pathogen-free conditions. Protocols were approved by the Institutional Animal Care and Use Committee of the University of Occupational and Environmental Health.

Statistical Analysis

Data were analyzed using an unpaired two-tailed *t*-test. A *P* value of less than 0.05 was considered to be significant.

Results

Increased S-G2 Phase in Fibroblasts of PDP

Case 1 had a typical complete form of PDP (Figure 1, A and B) characterized by the triad of pachydermia, digital clubbing, and periostosis.[1–3] The histology of the skin showed thickened dermis with dense and packed collagen and elastic fibers (Figure 1, C–E), suggesting that the function of fibroblasts was enhanced in PDP. To test the proliferative activity of fibroblasts, we cultured primary fibroblasts from case 1 and a matched control, and monitored their number. As reported previously,[26] the number of PDP fibroblasts was significantly higher than that of control fibroblasts (Figure 2A). Similar results were obtained in another typical patient with PDP, case 2 (data not shown). To clarify whether it was due to enhanced cell survival or proliferation, we stained the nuclear contents of fibroblasts with 7-AAD for cell cycle analysis. The ratio of PDP fibroblasts in the cell cycle (S-G2 phase) was higher than that of control fibroblasts (Figure 2B), suggesting that the proliferation of fibroblasts was enhanced in PDP.

Decreased DKK1 Expression in PDP Fibroblasts and Skin

The above results together with the clinical phenotypes involving the skin and bone suggested the possibility that the pathogenesis of PDP is related to dysregulation of BMP, Wnt, and/or TGF-β pathways in mesenchymal cells. To efficiently compare the expression profiles of these genes between PDP fibroblasts (case 1) and matched controls,

DNA microarray analysis was performed and the complete array data were deposited in a MIAME-compliant microarray database (GSE17947). Among all genes analyzed, 2573 genes were elevated and 2346 genes were decreased more than twofold in PDP patients compared with a healthy control. The analysis revealed that the mRNA levels of *BMP* and *TGF-β* families were comparable between these two groups (Table 2). On the other hand, *WNT1*, *WNT10B*, and *DKK1* mRNAs were decreased in the patient's fibroblasts (Table 2). In particular, *DKK1* mRNA was markedly decreased. Other molecules, such as levels of *LRP5/6*, *Kremen1*, and *Kremen2* mRNA were similar between these two groups (Table 2). Moreover, the mRNA levels for collagen families, such as *COL4A5*, *COL9A2*, *COL10A1*, *COL11A1*, *COL12A1*, *COL14A1*, and *COL17A1*, were elevated, but those for *fibronectin* and *elastin* (*ELN*) families were not (Table 2). These data suggest that the PDP fibroblasts showed enhanced production of several types of collagens in addition to cell proliferation, which might explain the pathogenesis of pachydermia in PDP.

We initially confirmed the decreased *DKK1* expression using quantitative RT-PCR. Fibroblasts were primarily cultured from two PDP patients (cases 1 and 2) and two matched healthy controls. *DKK1* mRNA levels in PDP fibroblasts were consistently lower than those in the control fibroblasts (Figure 2C). We then performed immunohistochemical analysis to evaluate the expression of DKK1 protein in the PDP skin (case 1) and the control. In the normal skin, DKK1 was detected diffusely in the dermis (Figure 2D, upper panels) and notably in the cytoplasm of fibroblasts (Figure 2D, lower panels). The intensity of this expression pattern was substantially decreased in the PDP patient (case 1) (Figure 2D, lower panels). This finding was confirmed with the other PDP patient (case 2) and another matched control (data not shown). We displayed that the controls incorporating non-immune serum (inset, Figure 2D) or mouse IgG1 (inset, Figure 2E) show no specific reactivity.

The decreased expression of DKK1 in PDP suggested that Wnt signaling is enhanced in PDP. Immunohistochemical analysis revealed enhanced β-catenin expression in the PDP skin (case 1), especially around the sebaceous glands, the hair follicles, and the epidermis, and mildly in the dermis, as compared with the control (Figure 2E), supporting the augmented expression of Wnt signaling.

Suppression of Fibroblast Proliferation by DKK1

The above results indicated that Wnt signaling is enhanced in PDP through decreased DKK1 expression. However, it was still unknown whether DKK1 directly modulates the function of dermal fibroblasts. To solve this issue, we cultured dermal fibroblasts from a healthy control and the patient with PDP (case 1) in the presence or absence of human recombinant DKK1, and quantitated the DNA contents of fibroblasts by cell cycle analysis with 7-AAD. The ratio of fibroblasts in the cell cycle (S-G2 phase) was higher in the PDP patient than in the control (Figure 3, A and B). In addition, the ratio of fibroblasts with the cell cycle (S-G2 phase) was decreased by treatment with recombinant DKK1 protein in a dose-dependent manner (Figure 3B), implicating the direct involvement of DKK1 in fibroblast proliferation.

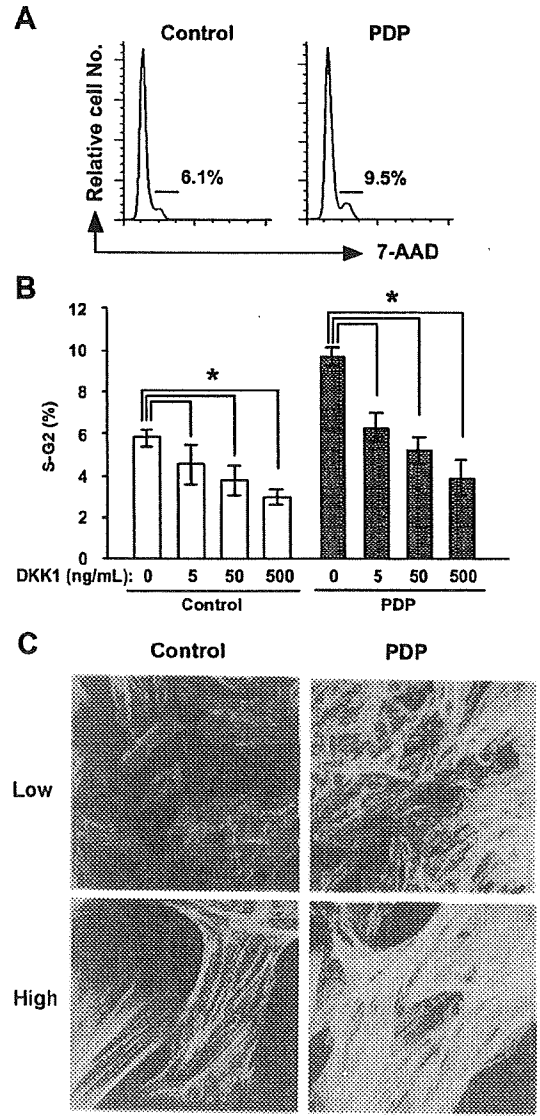

Figure 3. The effect of DKK1 on fibroblast proliferation and actin bundle formation of fibroblasts. **A, B:** The fibroblasts from a healthy individual (control) and an individual with PDP (PDP) were incubated with or without recombinant human DKK1 protein and the DNA contents of fibroblasts were evaluated with 7-AAD using flow cytometry. Representatives of FACS plots of fibroblasts from a healthy individual (control) and an individual with PDP (PDP) are shown (**A**). The percentages of fibroblasts in S-G2 phase in triplicated wells are expressed as the mean ± SD ($n = 3$). The student's *t*-test was performed between the indicated groups and $^*P < 0.05$. **C:** The actin bundle formation of cultured fibroblasts from a healthy individual (control) and an individual with PDP (PDP) were examined by staining with alexa 488-labeled phalloidin antibody 5 days after the fourth passage. Upper panels, low magnification (×10); lower panels, high magnification (×40).

Enhanced Actin Bundle Formation of Fibroblasts in PDP

Wnt signaling is also known to induce cell motility and cytoskeletal rearrangement of NIH3T3, a fibroblast cell line [27] Therefore, we examined the actin bundle formation

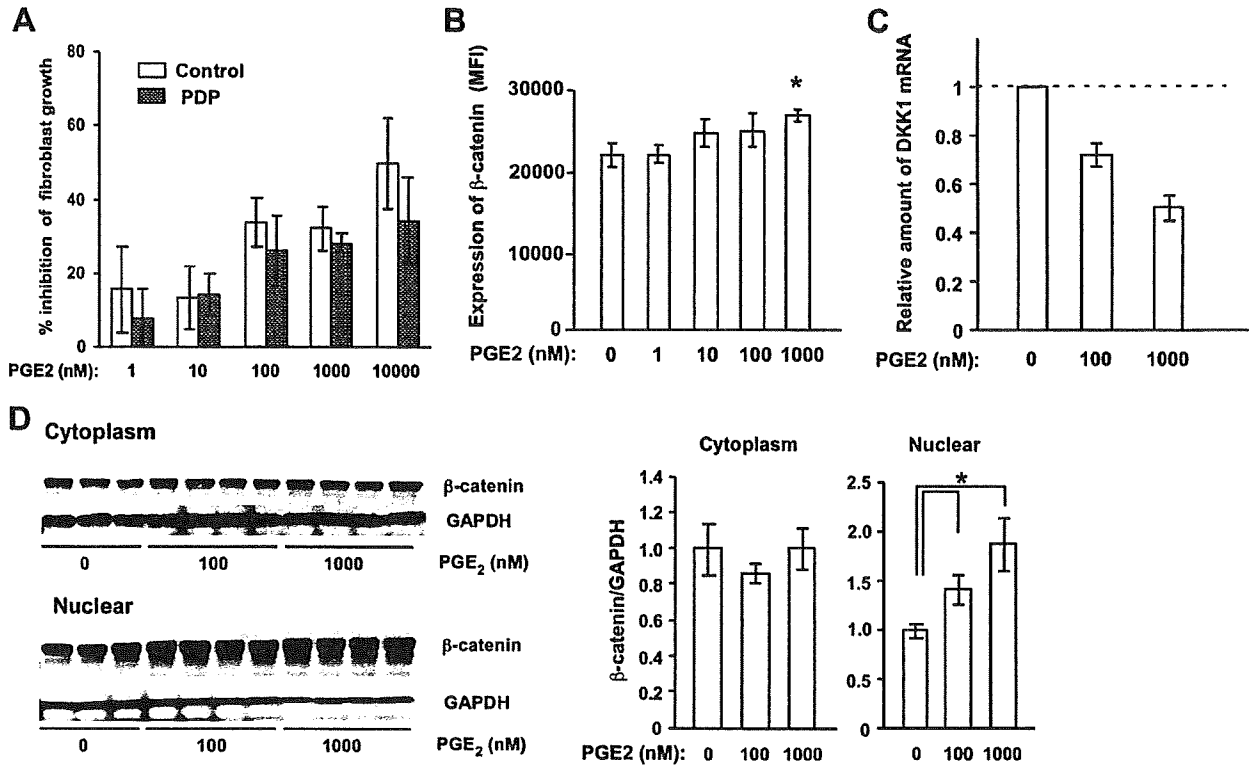

Figure 4. Effect of PGE_2 on fibroblasts. **A:** The % inhibition of the number of fibroblasts from a healthy donor and a PDP patient by the addition of PGE_2 was evaluated as (Number of fibroblasts without PGE_2 − Number of fibroblasts with PGE_2)/Number of fibroblasts without PGE_2 × 100. The growth inhibitory effect of PGE_2 is dose-dependent and comparable between these two groups. The values are expressed as the mean ± SD ($n = 3$) and are representative of two independent experiments. **B, C:** The effects of PGE_2 on β-catenin expression and *DKK1* mRNA levels in fibroblasts were evaluated. The mean fluorescent intensity (MFI) of β-catenin (**B**) and *DKK1* mRNA (**C**) in fibroblasts after exposure to PGE_2 is shown. The amount of *DKK1* mRNA relative to *GAPDH* mRNA without the addition of PGE_2 is regarded as one. The values are expressed as the mean ± SD ($n = 3$) and $^*P < 0.05$. **D:** Cytoplasm- (right panel) and nuclear- (left panel) protein samples from fibroblasts treated with or without 0, 100, and 1000 nmol/L PGE_2 for 4 days were used to determine the effect of PGE_2 on β-catenin expression. The values are expressed as the mean ± SD ($n = 3$ to 4) and $^*P < 0.05$.

of cultured fibroblasts with phalloidin staining 5 days after the fourth passage. Fluorescent microscopy showed that the actin bundle formation of PDP fibroblasts is promoted in PDP, as the bundles were thicker and denser than those of control fibroblasts (Figure 3C).

Effect of PGE_2 on Fibroblasts

It was recently reported that the incomplete form of PDP is induced by elevated PGE_2 due to a mutation in the *HPGD* gene.[6] If this PGE_2 alteration also affects pachydermia, PGE_2 would be expected to enhance fibroblast function and proliferation. The addition of PGE_2 into the cultured medium of fibroblasts decreased the number of dermal fibroblasts from healthy donors in a dose-dependent manner as reported previously[28,29] (Figure 4A). A similar effect was observed when PGE_2 was added to the culture medium of fibroblasts from the PDP patient (case 2). To examine whether PGE_2 affects Wnt signaling in fibroblasts, we measured the amount of β-catenin in fibroblasts after exposure to PGE_2 by flow cytometry, and found that β-catenin was significantly increased in fibroblasts by the addition of PGE_2 at a dose of 1000 nmol/L (Figure 4B). In addition, the mRNA expression level of *DKK1* was significantly decreased by the addition of PGE_2 at a dose of 100 and 1000 nmol/L (Figure 4C). Moreover, to determine the effect of PGE_2 on β-catenin expression, cytoplasm- and nuclear-protein samples were prepared from fibroblasts treated with or without 0, 100, and 1000 nmol/L PGE_2 in the presence of 10 μmol/L indomethacin for 4 days. In the cytoplasm, β-catenin expression was unchanged irrespective of the addition of PGE_2. However, β-catenin expression in the nuclei was significantly increased by the treatment with 100 and 1000 nmol/L PGE_2 (Figure 4D). These results suggest that PGE_2 signaling increases nuclear β-catenin in fibroblasts.

Genetic Analysis for DKK1, TCF-4, *and* HPGD *Genes*

To address the cause of PDP, we initially analyzed the sequences of *HPGD*, and found no mutation including single nucleotide polymorphism that was different among three healthy donors and two PDP patients (data not shown). Rather, our current results suggest that the pathogenesis of the complete form of PDP may be attributable to enhanced Wnt signaling secondary to decreased DKK1 expression. Moreover, it remains uncertain how DKK1 expression is reduced in PDP. One possible mediator is TCF7L2 (TCF-4), which binds to the *DKK1* promoter, thus enhancing activity of DKK1[30]

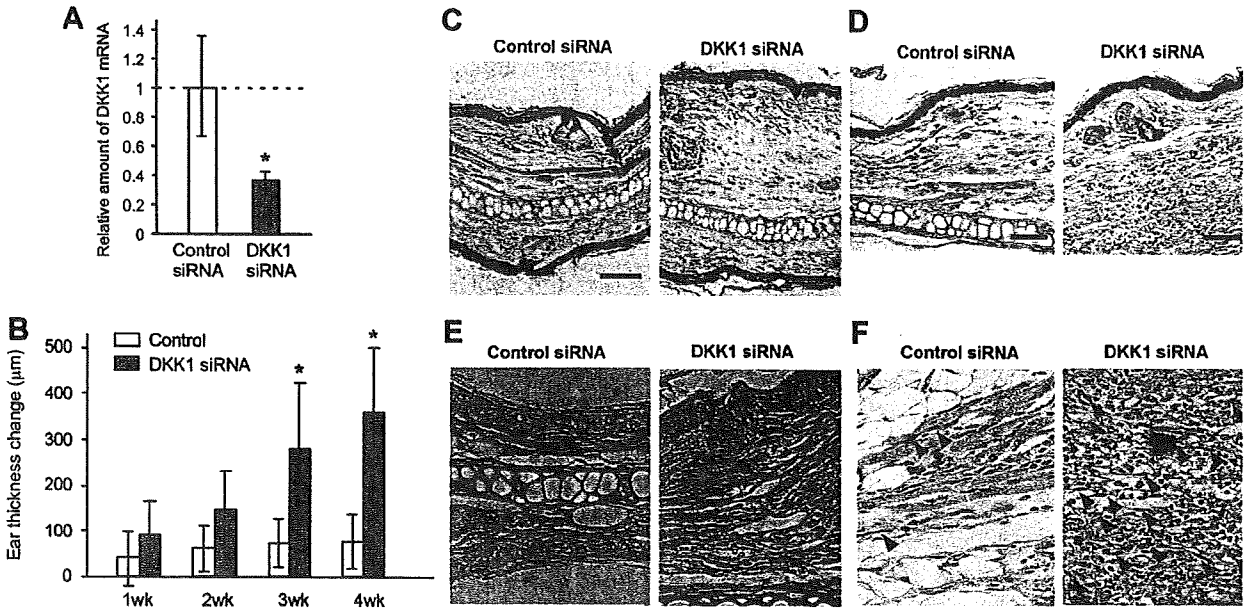

Figure 5. The effect of mouse *DKK1* siRNA on pachydermia. **A:** Mouse *DKK1* siRNA and control-scrambled siRNA (control siRNA) solutions were injected intradermally into the ears of mice four times every 7 days. The expression of *DKK1* mRNA in the skin 1 week after the last siRNA injection was evaluated by quantitative RT-PCR analysis. The mean value of *DKK1* mRNA relative to *GAPDH* mRNA treated with scrambled siRNA is regarded as one ($n = 5$). **B:** The ear thickness was measured every week before each injection and one week after the last injection. Columns show the mean ± *SD* ($n = 8$, each group) from two independent experiments. The student's *t*-test was performed between the indicated groups and $^*P < 0.05$. **C–D:** The skin from the ears one week after the last siRNA injection was fixed and stained with H&E (**C**). In addition, skin sections were stained with anti-β-catenin antibody by immunohistochemistry. Enhanced β-catenin expression is visible diffusely in the dermis of the skin treated with *DKK1* siRNA (**D**). Scale bars = 100 μm. **E:** The samples stained with Elastica van Gieson shows the thick collagen and elastic fibers in the dermis of mice treated with DKK1 siRNA. **F:** The samples are stained with proliferating cellular nuclear antigen (PCNA). **Red arrowheads** depict PCNA positive cells.

Hence, we further analyzed the sequence of *DKK1* and *TCF-4*. However, sequence analyses of the coding sequences of DKK1 and TCF-4, including exon-intron boundaries revealed no mutation (data not shown). In addition, the primers used in this study sequenced all exon-intron boundaries of *DKK1*, *TCF4*, and *HPGD*, but no mutation was found.

DKK1 *siRNA Enhances Ear Thickness in Mice*

Finally, we used mice to pursue direct evidence for DKK1 involvement in pachydermia. We injected a solution of mouse *DKK1* siRNA or control siRNA intradermally into the ears of mice four times every 7 days. Quantitative RT-PCR analysis revealed that this procedure successfully suppressed the expression of *DKK1* mRNA in the skin by about 60% (Figure 5A). The ear thickness was measured every week before each injection and 1 week after the last injection. The ear thickness was significantly augmented by the application of *DKK1* siRNA (Figure 5B). The histological findings showed that the dermis was thickened with increased fibroblasts (Figure 5, C–F). Consistent with these findings, enhanced β-catenin expression was observed diffusely in the dermis treated with *DKK1 si*RNA. (Figure 5D).

Discussion

We showed that Wnt/DKK1 plays a key role in the development of pachydermia in several aspects. Firstly, proliferation of fibroblasts from the PDP patients was promoted with a higher ratio in the cell cycle than compared with normal fibroblasts, and human recombinant DKK1 protein decreased their proliferation. Secondly, the expression levels of DKK1 mRNA in PDP fibroblasts and DKK1 protein in PDP skin were lower than those in healthy controls. Thirdly, β-catenin intensity in the skin from PDP was pronounced by immunohistochemistry. Finally, application of mouse *DKK1* siRNA increased the thickness of the skin in accordance with the elevated β-catenin levels. These results suggest that enhanced Wnt signaling is related to the development of pachydermia.

Pachydermia is one of the clinical manifestations of the complete form of PDP, which involves both skin and bone. For example, BMP, TGF-β, and Wnt families are the possible molecules responsible for the changes in both organs. There are several congenital diseases related to both organs, such as basal cell nevus syndrome, synovitis acne pustulosis hyperostosis ostitis syndrome, Klippel-Trenaunay-Weber syndrome, and Buschke-Ollendorff syndrome.[31–33] Bushchke-Ollendorff syndrome, in which osteopoikilosis is associated with connective tissue nevi, is particularly of note, since mutations in *LEMD3*, a gene implicated in BMP signaling, are candidates for its pathogenesis.[34] However, we could not detect a significant difference in mRNA expression for *BMP* or *TGF-β* families between PDP and control fibroblasts by DNA microarray analysis.

Recently, the incomplete form of PDP was attributed to elevated PGE_2 due to the mutation of *HPGD*. The skeletal phenotype of PDP, particularly clubbing and periostosis, can clearly be explained by elevated PGE_2, since it is well known that PGE_2 stimulates the activity of both os-

teoclasts and osteoblasts,[35] leading to bone deposition (periostosis) and resorption (acro-osteolysis), respectively. However, we could not detect a mutation in HPGD. In addition, the level of serum PGE_2 from one of our PDP cases (case 1) was within the normal range (data not shown). In fact, long-term therapeutic administration of exogenous PGE_2 for skin ulcers secondary to systemic sclerosis, arteriosclerosis obliterans, and Buerger diseases does not induce pachydermia, sebaceous hyperplasia, or velvet coloration of the skin as adverse effects. Moreover, the addition of PGE_2 into the fibroblast culture did not induce proliferation. Therefore, it remains unknown how the skin manifestations of PDP are induced.

Here we focused on Wnt signaling in the development of pachydermia. Fibroblasts from PDP skin and bone marrow-derived fibroblasts of PDP patients are known to grow faster than those of healthy donors.[26,36] The transfection of *DKK1* into cultured mouse fibroblasts, NIH3T3, blocked WNT2-induced cell growth and the WNT2-induced increase in uncomplexed β-catenin.[37] WNT3a induced motility and cytoskeletal rearrangement of NIH3T3 cells.[27] These previous reports suggest that enhanced Wnt/β-catenin signaling promotes fibroblast proliferation and cytoskeletal rearrangement. In fact, we found that the frequency of PDP fibroblasts in cycle was increased, and that actin bundle formation was more pronounced in PDP fibroblasts. Moreover, the addition of human recombinant *DKK1* consistently suppressed the fibroblast proliferation.

The source of DKK1 and how it works in the skin are issues that remain to be clarified. According to our immunohistochemical analysis, the major source of DKK1 in the skin seems to be fibroblasts, because the DKK1 expression in fibroblasts was low in PDP. Since DKK1 is a secreted antagonist and may affect bystander cells in the vicinity of fibroblasts, the dysregulated production of DKK1 possibly modulates the functions of not only fibroblasts but also other cells, such as keratinocytes and melanocytes. It was reported that high *DKK1* expression by dermal fibroblasts in the palms and soles inhibits the function of melanocytes via suppression of β-catenin and microphthalmia-associated transcription factor, and enhances keratinocyte proliferation.[16,17,38] Mice with an overexpression of *DKK1* in skin consistently lacked formation of appendages, such as hair follicles, and the mice had no skin pigmentation on the trunk.[18]

The role of DKK1 has been more extensively studied in bone than in the skin. DKK1 is known to inhibit osteoblast differentiation, and the overproduction of DKK1 was noted in osteolytic bone lesions of patients with multiple myeloma.[39] The elevated *DKK1* levels in bone marrow plasma and peripheral blood from the patients were correlated with the presence of focal bone lesions. Recombinant human *DKK1* inhibited the differentiation of osteoblast precursor cells *in vitro*.[40,41] These previous observations could explain the periostosis in PDP possibly secondary to decreased *DKK1* expression. Since fibroblasts and osteoblasts are derived from mesenchymal origin, they seem to share in common the mechanism of differentiation and proliferation. Although we did not address the relationship between DKK1 and the skeletal phenotype in PDP, it would be of interest to analyze the function of osteoblasts in PDP.

The next question is how Wnt signaling is enhanced. One possibility provided by our present study is the suppression of DKK1 expression in fibroblasts. The mechanism by which DKK1 is down-regulated in PDP remains to be elucidated. It can be hypothesized that there is a mutation in *DKK1* or molecules controlling *DKK1* expression, such as TCF-4. However, no mutation was detected in either exons of DKK1 or TCF-4 genes. Therefore, in the present study, we could not determine the genetic mechanism responsible for the complete form of PDP and/or pachydermia. Given the defect in PDP appears to altered expression of DKK1, it will be of interest in future studies to analyze the regulatory regions of DKK1, especially around the TCF binding sites, an issue which remains to be clarified.

On the other hand, the Wnt/β-catenin pathway is known to increase *DKK1* mRNA and protein, thus initiating a negative feedback loop.[42] It can be hypothesized that this negative feedback regulation might be dysregulated in PDP. Moreover, due to this negative feedback system, DKK1 can work as a tumor suppressor gene in some types of neoplasia.[42,43] Hypertrophic osteoarthritis is occasionally induced by a variety of thoracoabdominal, sometimes malignant, conditions. The relationship between decreased DKK1 expression and secondary hypertrophic osteoarthritis in association with malignancy may be an interesting issue to pursue.

It still remains unclear whether PDP in our cases could be attributed to the mutation in HPGD or not. Of note is that our cases were diagnosed as the complete form of PDP including pachydermia and adolescent onset, but that the cases with HPGD mutation had the incomplete form of PDP without pachydermia and with early onset (within the first year of their lives). The onset of the PDP is bimodal. The first peak is during the first year of the life and the second at the age of 15 years.[3,44] Therefore, the pathogenesis of PDP might be subdivided into at least two groups. However, further clinical studies in combination with HPGD mutation analysis will be required to clarify this.

In PDP, clinical cutaneous manifestations include pachydermia, seborrhea, and velvet colored skin. At present, we could not show direct evidence that all of the phenotypes of PDP were induced by enhanced Wnt signaling secondary to the suppressed expression of DKK1. In addition, the number of cases in our study was limited. However, our findings, together with those of previous studies suggest that the Wnt signaling pathway was promoted in accordance with decreased DKK1 expression, leading to increased fibroblast proliferation, enhanced pigmentation of the skin, and adnexal hyperplasia.

Acknowledgments

We thank Ms Rie Murase and Dr. Yosuke Okada for technical assistance, and Dr. Tatsuya Ishibe for discussion.

References

1. Vogl A, Goldfischer S: Pachydermoperiostosis: primary or idiopathic hypertrophic osteoarthropathy. Am J Med 1962, 33:166–187
2. Shawarby K, Ibrahim MS: Pachydermoperiostosis. A review of literature and report on four cases. Br Med J 1962, 1:763–766
3. Rimoin DL: Pachydermoperiostosis (idiopathic clubbing and periostosis): genetic and physiologic considerations. N Engl J Med 1965, 272:923–931
4. Jajic I, Jajic Z, Grazio S: Minor but important symptoms and signs in primary hypertrophic osteoarthropathy. Clin Exp Rheumatol 2001, 19:357–358
5 Touraine A, Solente G, Gole A: Un syndrome osteodermopathique: la pachydermie plicaturee avec pachyperiostose des extremites. Presse Med 1935, 43:1820–1824
6. Uppal S, Diggle CP, Carr IM, Fishwick CW, Ahmed M, Ibrahim GH, Helliwell PS, Latos-Bielenska A, Phillips SE, Markham AF, Bennett CP, Bonthron DT: Mutations in 15-hydroxyprostaglandin dehydrogenase cause primary hypertrophic osteoarthropathy. Nat Genet 2008, 40: 789–793
7. Castori M, Sinibaldi L, Mingarelli R, Lachman RS, Rimoin DL, Dallapiccola B: Pachydermoperiostosis: an update. Clin Genet 2005, 68:477–486
8. Kornak U, Mundlos S: Genetic disorders of the skeleton: a developmental approach. Am J Hum Genet 2003, 73:447–474
9. Botchkarev VA, Sharov AA: BMP signaling in the control of skin development and hair follicle growth. Differentiation 2004, 72:512–526
10. Zorn AM: Wnt signalling: antagonistic Dickkopfs. Curr Biol 2001, 11:R592–595
11. Kawano Y, Kypta R: Secreted antagonists of the Wnt signalling pathway. J Cell Sci 2003, 116:2627–2634
12. Mao B, Wu W, Davidson G, Marhold J, Li M, Mechler BM, Delius H, Hoppe D, Stannek P, Walter C, Glinka A, Niehrs C: Kremen proteins are Dickkopf receptors that regulate Wnt/beta-catenin signalling. Nature 2002, 417:664–667
13. Mao B, Wu W, Li Y, Hoppe D, Stannek P, Glinka A, Niehrs C: LDL-receptor-related protein 6 is a receptor for Dickkopf proteins. Nature 2001, 411:321–325
14. Glinka A, Wu W, Delius H, Monaghan AP, Blumenstock C, Niehrs C: Dickkopf-1 is a member of a new family of secreted proteins and functions in head induction. Nature 1998, 391:357–362
15. Grotewold L, Ruther U: The Wnt antagonist Dickkopf-1 is regulated by Bmp signaling and c-Jun and modulates programmed cell death. EMBO J 2002, 21:966–975
16. Yamaguchi Y, Itami S, Watabe H, Yasumoto K, Abdel-Malek ZA, Kubo T, Rouzaud F, Tanemura A, Yoshikawa K, Hearing VJ: Mesenchymal-epithelial interactions in the skin: increased expression of dickkopf1 by palmoplantar fibroblasts inhibits melanocyte growth and differentiation. J Cell Biol 2004, 165:275–285
17. Yamaguchi Y, Passeron T, Watabe H, Yasumoto K, Rouzaud F, Hoashi T, Hearing VJ: The effects of dickkopf 1 on gene expression and Wnt signaling by melanocytes: mechanisms underlying its suppression of melanocyte function and proliferation. J Invest Dermatol 2007, 127:1217–1225
18. Andl T, Reddy ST, Gaddapara T, Millar SE: WNT signals are required for the initiation of hair follicle development. Dev Cell 2002, 2:643–653
19. Masuda K, Moriwaki S, Takigawa M, Furukawa F, Higashishiba T, Fukamizu H: A case of pachydermoperiostosis. Rinsho Hifuka (Japanese) 2000, 54:398–401
20 Kabashima K, Banks TA, Ansel KM, Lu TT, Ware CF, Cyster JG: Intrinsic lymphotoxin-beta receptor requirement for homeostasis of lymphoid tissue dendritic cells. Immunity 2005, 22:439–450
21. Kabashima K, Haynes NM, Xu Y, Nutt SL, Allende ML, Proia RL, Cyster JG: Plasma cell S1P1 expression determines secondary lymphoid organ retention versus bone marrow tropism. J Exp Med 2006, 203:2683–2690
22. Livak KJ, Schmittgen TD: Analysis of relative gene expression data using real-time quantitative PCR and the 2[-Delta Delta C(T)] method. Methods 2001, 25:402–408
23 Kabashima K, Sakabe J, Yamada Y, Tokura Y: "Nagashima-type" keratosis as a novel entity in the palmoplantar keratoderma category. Arch Dermatol 2008, 144:375–379
24. Maekawa M, Yamamoto T, Tanoue T, Yuasa Y, Chisaka O, Nishida E: Requirement of the MAP kinase signaling pathways for mouse preimplantation development. Development 2005, 132:1773–1783
25 Kushibiki T, Matsumoto K, Nakamura T, Tabata Y: Suppression of tumor metastasis by NK4 plasmid DNA released from cationized gelatin. Gene Ther 2004, 11:1205–1214
26 Matucci-Cerinic M, Sacerdoti L, Perrone C, Carossino A, Cagnoni ML, Jajic I, Lotti T: Pachydermoperiostosis (primary hypertrophic osteoarthropathy): in vitro evidence for abnormal fibroblast proliferation. Clin Exp Rheumatol 1992, 10 Suppl 7:57–60
27. Kim SE, Choi KY: EGF receptor is involved in WNT3a-mediated proliferation and motility of NIH3T3 cells via ERK pathway activation. Cell Signal 2007, 19:1554–1564
28. Fine A, Goldstein RH: The effect of PGE2 on the activation of quiescent lung fibroblasts. Prostaglandins 1987, 33:903–913
29. Korn JH, Halushka PV, LeRoy EC: Mononuclear cell modulation of connective tissue function: suppression of fibroblast growth by stimulation of endogenous prostaglandin production. J Clin Invest 1980, 65:543–554
30. Niida A, Hiroko T, Kasai M, Furukawa Y, Nakamura Y, Suzuki Y, Sugano S, Akiyama T: DKK1, a negative regulator of Wnt signaling, is a target of the beta-catenin/TCF pathway. Oncogene 2004, 23:8520–8526
31 Kahn MF, Chamot AM: SAPHO syndrome. Rheum Dis Clin North Am 1992, 18:225–246
32. Oduber CE, van der Horst CM, Hennekam RC: Klippel-Trenaunay syndrome: diagnostic criteria and hypothesis on etiology. Ann Plast Surg 2008, 60:217–223
33. Ehrig T, Cockerell CJ: Buschke-Ollendorff syndrome: report of a case and interpretation of the clinical phenotype as a type 2 segmental manifestation of an autosomal dominant skin disease. J Am Acad Dermatol 2003, 49:1163–1166
34. Hellemans J, Preobrazhenska O, Willaert A, Debeer P, Verdonk PC, Costa T, Janssens K, Menten B, Van Roy N, Vermeulen SJ, Savarirayan R, Van Hul W, Vanhoenacker F, Huylebroeck D, De Paepe A, Naeyaert JM, Vandesompele J, Speleman F, Verschueren K, Coucke PJ, Mortier GR: Loss-of-function mutations in LEMD3 result in osteopoikilosis, Buschke-Ollendorff syndrome and melorheostosis. Nat Genet 2004, 36:1213–1218
35 Raisz LG, Pilbeam CC, Fall PM: Prostaglandins: mechanisms of action and regulation of production in bone. Osteoporos Int 1993, 3 Suppl 1:136–140
36. Fontenay-Roupie M, Dupuy E, Berrou E, Tobelem G, Bryckaert M: Increased proliferation of bone marrow-derived fibroblasts in primitive hypertrophic osteoarthropathy with severe myelofibrosis. Blood 1995, 85:3229–3238
37. Fedi P, Bafico A, Nieto Soria A, Burgess WH, Miki T, Bottaro DP, Kraus MH, Aaronson SA: Isolation and biochemical characterization of the human Dkk-1 homologue, a novel inhibitor of mammalian Wnt signaling. J Biol Chem 1999, 274:19465–19472
38. Yamaguchi Y, Passeron T, Hoashi T, Watabe H, Rouzaud F, Yasumoto K, Hara T, Tohyama C, Katayama I, Miki T, Hearing VJ: Dickkopf 1 (DKK1) regulates skin pigmentation and thickness by affecting Wnt/beta-catenin signaling in keratinocytes. FASEB J 2008, 22:1009–1020
39. Qiang YW, Endo Y, Rubin JS, Rudikoff S: Wnt signaling in B-cell neoplasia. Oncogene 2003, 22:1536–1545
40. Tian E, Zhan F, Walker R, Rasmussen E, Ma Y, Barlogie B, Shaughnessy JD Jr: The role of the Wnt-signaling antagonist DKK1 in the development of osteolytic lesions in multiple myeloma. N Engl J Med 2003, 349:2483–2494
41. Morvan F, Boulukos K, Clement-Lacroix P, Roman Roman S, Suc-Royer I, Vayssiere B, Ammann P, Martin P, Pinho S, Prognonec P, Mollat P, Niehrs C, Baron R, Rawadi G: Deletion of a single allele of the Dkk1 gene leads to an increase in bone formation and bone mass. J Bone Miner Res 2006, 21:934–945
42 Gonzalez-Sancho JM, Aguilera O, Garcia JM, Pendas-Franco N, Pena C, Cal S, Garcia de Herreros A, Bonilla F, Munoz A: The Wnt antagonist DICKKOPF-1 gene is a downstream target of beta-catenin/TCF and is downregulated in human colon cancer. Oncogene 2005, 24:1098–1103
43 Polakis P: Wnt signaling and cancer. Genes Dev 2000, 14:1837–1851
44 Matucci-Cerinic M, Lotti T, Jajic I, Pignone A, Bussani C, Cagnoni M: The clinical spectrum of pachydermoperiostosis (primary hypertrophic osteoarthropathy). Medicine (Baltimore) 1991, 70:208–214

Activated regulatory T cells are the major T cell type emigrating from the skin during a cutaneous immune response in mice

Michio Tomura,[1] Tetsuya Honda,[2] Hideaki Tanizaki,[2] Atsushi Otsuka,[2] Gyohei Egawa,[2,3] Yoshiki Tokura,[4] Herman Waldmann,[5] Shohei Hori,[6] Jason G. Cyster,[7] Takeshi Watanabe,[3] Yoshiki Miyachi,[2] Osami Kanagawa,[1] and Kenji Kabashima[2,3]

[1]Laboratory for Autoimmune Regulation, Research Center for Allergy and Immunology, RIKEN, Yokohama City, Japan. [2]Department of Dermatology and [3]Center for Innovation in Immunoregulative Technology and Therapeutics, Kyoto University Graduate School of Medicine, Japan. [4]Department of Dermatology, University of Occupational and Environmental Health, Kitakyushu, Japan. [5]Sir William Dunn School of Pathology, Oxford, United Kingdom. [6]Research Unit for Immune Homeostasis, Research Center for Allergy and Immunology, RIKEN. [7]Howard Hughes Medical Institute and Department of Microbiology and Immunology, UCSF, San Francisco, California.

Tregs play an important role in protecting the skin from autoimmune attack. However, the extent of Treg trafficking between the skin and draining lymph nodes (DLNs) is unknown. We set out to investigate this using mice engineered to express the photoconvertible fluorescence protein Kaede, which changes from green to red when exposed to violet light. By exposing the skin of Kaede-transgenic mice to violet light, we were able to label T cells in the periphery under physiological conditions with Kaede-red and demonstrated that both memory phenotype $CD4^+Foxp3^-$ non-Tregs and $CD4^+Foxp3^+$ Tregs migrated from the skin to DLNs in the steady state. During cutaneous immune responses, Tregs constituted the major emigrants and inhibited immune responses more robustly than did LN-resident Tregs. We consistently observed that cutaneous immune responses were prolonged by depletion of endogenous Tregs in vivo. In addition, the circulating Tregs specifically included activated $CD25^{hi}$ Tregs that demonstrated a strong inhibitory function. Together, our results suggest that Tregs in circulation infiltrate the periphery, traffic to DLNs, and then recirculate back to the skin, contributing to the downregulation of cutaneous immune responses.

Introduction

Lymphocytes travel throughout the body to conduct immune surveillance. $CD4^+$ helper T cells are central organizers in immune responses. Upon stimulation, naive $CD4^+$ T cells differentiate into effector Th cells (1). $Foxp3^+$ Tregs represent a unique subpopulation of $CD4^+$ T cells that are important for maintenance of immunological homeostasis and self tolerance (2, 3). Naive T cells circulate between blood and secondary lymphoid tissues (4–7). However, it is debatable whether T cells travel through uninflamed peripheral tissues as part of their recirculation route. One type of peripheral tissue with the active afferent limb of the lymphatic system is, for example, the skin, and memory/effector T cells migrate to inflamed skin using CCR4 and CCR10 (8–10). Classic studies employing cannulation of afferent lymph vessels have shown that $CD4^+$ memory/effector cells make up nearly all cells in the afferent lymph of sheep (6, 11–13). On the other hand, Debes et al. have reported that $CD4^+$ cells, especially naive subsets, migrate from the skin in a CCR7-dependent manner using subcutaneous injection of fluorescent-labeled lymphocytes (14). However, the above experiments require traumatic or artificial procedures to follow or label T cells. Therefore, it is of interest to clarify whether T cells in the peripheral organs such as the skin migrate to draining LNs (DLNs) and to identify the T cell subsets of migration and their roles under physiological conditions.

To directly assess cells migrating from the peripheral tissue, we have devised a new experimental system that involves labeling resident cells using Tg mice expressing the Kaede protein. Kaede is a photoconvertible green fluorescence protein cloned from stony coral (15, 16) that changes its color from green to red when exposed to violet light (16). Therefore, the Kaede-Tg mouse system is an ideal tool for monitoring precise cellular movements in vivo at different stages of the immune response (17).

Here, we used the skin as a representative of the peripheral organs and observed the movement of cells from the skin using Kaede-Tg mice (17). A high proportion of the migrating cells into the DLNs were Tregs that had a stronger capacity to suppress acquired immune responses than LN-resident Tregs. Moreover, these migrating T cells recirculated into the skin upon elicitation to terminate immune responses.

Results

Detection of cell migration from the skin in the steady state using Kaede-Tg mice. To monitor cell migration from the skin in vivo, the abdominal skin of Kaede-Tg mice was photoconverted by exposure to violet light for 10 minutes (see Methods). Before photoconversion, all the cells in the skin of Kaede-Tg mice expressed only Kaede-green fluorescence (Kaede-green) (Figure 1, A and B). Immediately after violet light exposure to the skin, the whole skin tissue (Supplemental Figure 1; supplemental material available online with this article; doi:10.1172/JCI40926DS1) and the skin cells of the photoconverted area showed red signal (Kaede-red), whereas virtually no draining axillary LN cells (Figure 1, A and B, and Supplemental Figure 2) or blood cells (Supplemental Figure 2)

Authorship note: Michio Tomura and Tetsuya Honda contributed equally to this work.

Conflict of interest: The authors have declared that no conflict of interest exists.

Citation for this article: *J Clin Invest.* 2010;120(3):883–893. doi:10.1172/JCI40926.

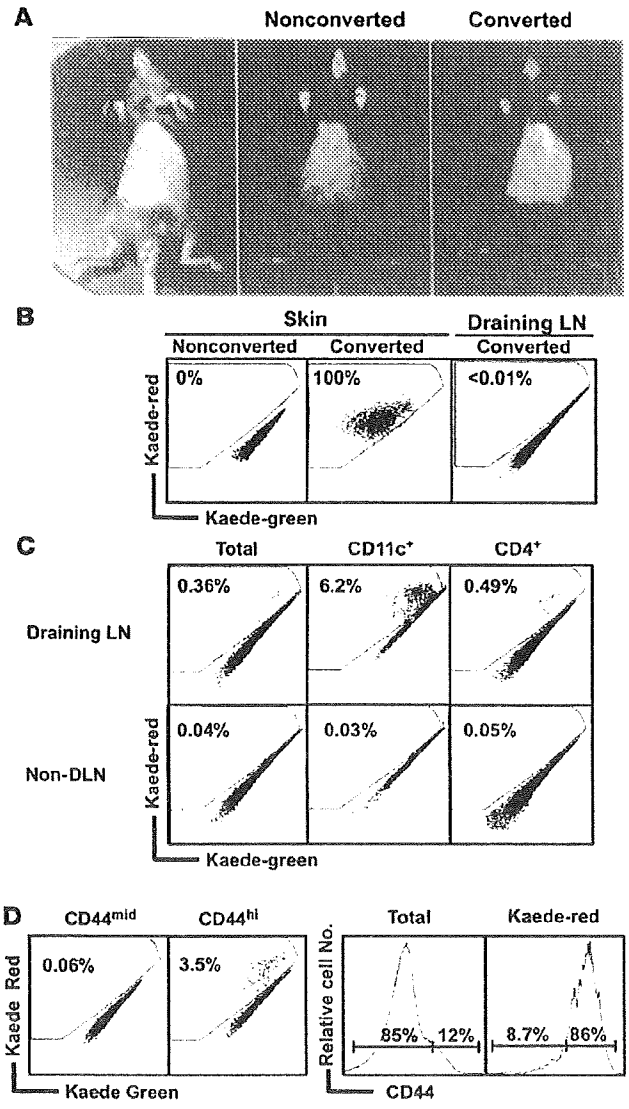

Figure 1

Cell migration from the skin to the DLN in the steady state. (**A**) Kaede-Tg mice were photoconverted on the clipped abdominal skin as described in Methods and observed with a fluorescence stereoscopic microscope. Nonphotoconverted clipped skin is shown as a control (middle). Note: nonclipped area remains black since light cannot reach. (**B**) Skin and draining axillary LN cells resected immediately after violet light exposure of the abdominal skin and resected skin cells not exposed to violet light were subjected to flow cytometric analysis to evaluate the photoconversion. (**C** and **D**) Twenty-four hours after photoconversion of the abdominal skin, cells from the draining axillary and other nondraining cervical and popliteal peripheral LNs were stained with CD11c and CD4 mAbs (**C**) and CD4 and CD44 mAbs (**D**) and subjected to flow cytometry. These data are representative of at least 5 experiments. Numbers within plots or histograms (**B**–**D**) indicate percentage of cells in the respective areas.

were photoconverted. Although we found that Kaede-red proteins could be detected in the extracellular fluids when incubated for 24 hours after photoconversion of the LN cells (Supplemental Figure 3), we confirmed that the extracellular photoconverted Kaede proteins could not be transferred into T cells in vitro (Supplemental Figure 4).

To evaluate cell migration from the skin in the steady state, the clipped abdominal skin of Kaede-Tg mice was exposed to violet light as in Figure 1A, and 24 hours later, the draining axillary and nondraining cervical and popliteal LN cells were subjected to flow cytometry. We found that 0.36% of the DLN cells showed the Kaede-red phenotype (Figure 1C), suggesting a fraction of cells in the skin migrate to the DLNs. It is generally thought that dendritic cells are the major migrants from the skin in the steady state, and in fact 6.2% of $CD11c^+$ dendritic cells were of the Kaede-red phenotype in the DLNs (Figure 1C). In contrast, almost no Kaede-red $CD11c^+$ dendritic cells were detected in the non-DLNs (Figure 1C). We next evaluated $CD4^+$ T cell migration from the skin and found that 0.49% of $CD3^+CD4^+$ T cells in the DLNs had the Kaede-red phenotype (Figure 1C). Although the frequencies of the Kaede-red positivity among dendritic cells and $CD3^+CD4^+$ T cells differed, the absolute numbers of Kaede-red dendritic cells and $CD4^+$ T cells were comparable ($CD4^+$ T cells vs. $CD11c^+$ dendritic cells: 11621 ± 2716 cells per LN vs. 9063 ± 2333 cells per LN, n = 5 each, average ± SD). Moreover, the ratio of Kaede-red cells was higher in $CD44^{hi}$ memory T cells than in $CD44^{mid}$ naive T cells (Figure 1D). Consistently, the majority of Kaede-red migratory cells were of the $CD44^{hi}$ memory phenotype (Figure 1D). These results suggest that predominantly T cells with the memory surface phenotype migrate from the skin into DLNs, even in the steady state.

Migration of Tregs from the skin to the DLNs. Immune responses and homeostasis are regulated by the functions of memory/effector T cells and Tregs. To determine the behaviors of these populations, we intercrossed Kaede-Tg mice with Foxp3 reporter mice expressing human CD2 and human CD52 chimeric protein, which are designated as Kaede/Foxp3$^{hCD2/hCD52}$ mice. Since $Foxp3^+$ cells coexpress hCD2 on the cell surface, live $Foxp3^+$ Tregs could be labeled and sorted with anti-hCD2 monoclonal Ab. The DLN cells from Kaede/Foxp3$^{hCD2/hCD52}$ mice in the steady state were analyzed by flow cytometry. A majority of $CD25^+$ cells were hCD2 positive, but a substantial number of $hCD2^+$ cells were detected even in $CD25^-$ cells (18) (Figure 2A), which is consistent with the previous findings by the other group (19). Therefore, the following studies were performed using Kaede/Foxp3$^{hCD2/hCD52}$ mice, and $hCD2^+$ cells were considered to be Tregs.

To evaluate T cell migration from the skin in the steady state, the clipped abdominal skin of Kaede/Foxp3$^{hCD2/hCD52}$ mice was exposed to violet light as in Figure 1A, and 24 hours later, the draining axillary LN cells were subjected to flow cytometry. Consistent with the previous results (Figure 1D), a substantial percentage (0.83%) of photoconverted $CD4^+$ T cells were observed in the DLNs (Figure 2B). Among $hCD2^-$ non-Tregs and $hCD2^+$ Tregs, the frequency of Kaede-red cells was comparable (0.79% vs. 0.98%) (Figure 2C), and the frequency of Kaede-red cells was higher in the $CD44^{hi}$ memory subset than in the $CD44^{mid}$ naive subset (Figure 2C). In addition, Kaede-red $CD4^+$ cells included a higher percentage of Tregs (22.7%) than total $CD4^+$ cells (14.1%) (Figure 2D). In total $CD4^+$ populations, the number of $CD44^{hi}$ memory cells was lower than that of $CD44^{mid}$ naive cells in both non-Tregs and Tregs (Figure 2E). In contrast, consistent with Figures 2C and 2D, $CD44^{hi}$ memory cells were the major Kaede-red migrants from the skin among non-Tregs and Tregs (Figure 2E).